Fluorescence Spectroscopic Profiling of Compound Libraries

Anton Simeonov, Ajit Jadhav, Craig J. Thomas, Yuhong Wang, Ruili Huang, Noel T. Southall, Paul Shinn, Jeremy Smith, Christopher P. Austin, Douglas S. Auld, and James Inglese*

NIH Chemical Genomics Center, National Human Genome Research Institute, National Institutes of Health, Bethesda, Maryland 20892-3370

Received October 16, 2007

Chromo/fluorophoric properties often accompany the heterocyclic scaffolds and impurities that comprise libraries used for high-throughput screening (HTS). These properties affect assay outputs obtained with optical detection, thus complicating analysis and leading to false positives and negatives. Here, we report the fluorescence profile of more than 70 000 samples across spectral regions commonly utilized in HTS. The quantitative HTS paradigm was utilized to test each sample at seven or more concentrations over a 4-log range in 1536-well format. Raw fluorescence was compared with fluorophore standards to compute a normalized response as a function of concentration and spectral region. More than 5% of library members were brighter than the equivalent of 10 nM 4-methyl umbelliferone, a common UV-active probe. Red-shifting the spectral window by as little as 100 nm was accompanied by a dramatic decrease in autofluorescence. Native compound fluorescence, fluorescent impurities, novel fluorescent compounds, and the utilization of fluorescence profiling data are discussed.

Introduction

The screening of small-molecule libraries against biological targets is now established as the predominant method by which bioactive compounds are identified. Modern methods of high-throughput screening (HTS)[1,a] library synthesis and compound management[2,3] have enabled these efforts, and novel techniques continue to be devised. Significant effort often follows HTS to validate compound activity prior to embarking on lead optimization.[4–8] Subsequent to HTS, steps are implemented to ensure that compound activities are mediated by relevant biological interactions rather than physico-chemical compound characteristics that lead to interference with particular assay systems. For example, the phenomenon of colloidal aggregation as a mechanism of nonspecific inhibition in HTS assays has been described in detail,[9] but there are numerous other interferences, such as inhibition of reporters (e.g., luciferase),[10] that can result in the selection of reproducible yet irrelevant active samples for follow-up.

Interference mediated by sample fluorescence is highly prevalent in HTS owing to the wide use of detection strategies performed with fluorescent labels and light detection in screening assay formats.[1] Assay artifacts arising from fluorescent compounds are reproducible, and the apparent activity will generally tend to display a concentration-dependent response. In this case, orthogonal assays are used to accept or reject the putative actives. Typically, such verification assays are conducted subsequently to the retesting of primary-screening actives. In HTS, attempts have been made to perform compound interference assessment by prereading the fluorescence intensity of the assay mixture after compound addition but prior to initiation of the assay that results in a change in the detection fluorophore (e.g., as in enzymatic assays before the addition of labeled profluorescent substrate). Preread measurements yield counter-screen data for fluorescent compounds within a near-identical assay milieu as the bioassay, because the same reader, settings, and microtiter plate are used. Retrospective assessment of the fluorescent interference from a given compound is possible in fluorescence polarization (FP)-based assays by combining the fluorescence intensity and computed polarization values for each well to incriminate samples with above-average fluorescence.[11–15] However, in systems such as competition-based FP, fluorescent interference can lead to equal and opposite effects on the relevant assay signal, resulting in false negatives. In recent years, accumulated anecdotal evidence of high levels of fluorescence interference being associated with assays and reporter fluorophores used in the UV-end of the light spectrum has prompted attempts to develop detection systems operating in the middle of the visible spectrum, as well as systems that do not depend directly on intensity measurements.[16–21]

The basic principles of fluorescence[22,23] are generally well understood, and although the fluorescence properties[24] of many small molecules are appreciated and catalogued,[25] these data are biased toward marketed fluorophores, which represent a small fraction of currently extant chemical matter and are not necessarily representative of chemical libraries used in HTS. Compounds identified as fluorescent in large screening campaigns are typically not disclosed because of concerns about proprietary structural and/or target information. A publicly available, unbiased, and comprehensive profile of fluorescence properties of a large compound collection would assist in the triaging and prioritization of HTS actives, identification of new fluorescent structural scaffolds, and understanding of the general principles of compound fluorescence.

In this study, we assess the fluorescent properties of the National Institutes of Health (NIH) Chemical Genomics Center (NCGC) screening collection, which includes the Molecular Libraries Small Molecule Repository (MLSMR) of the NIH Molecular Libraries Screening Center Network. The fluorescent measurements covered commonly used spectral regions, and by comparing the raw-fluorescence output from each sample with that of a set of calibration standards, we were able to relate

* To whom correspondence should be addressed. E-mail: jinglese@mail.nih.gov. Phone: 301-217-5723. Fax: 301-217-5736.

[a] Abbreviations: HTS, high-throughput screening; FP, fluorescence polarization; NIH, National Institutes of Health; NCGC, NIH Chemical Genomics Center; qHTS, quantitative high-throughput screening; HPLC, high-performance liquid chromatography; MLSMR, Molecular Libraries Small Molecule Repository; FEC, fluorophore-equivalent concentration; CCD, charge-coupled device; 4-MU, 4-methyl umbelliferone; SOM, self-organizing map; SRMLSC, Southern Research Molecular Libraries Screening Center; SAR, structure−activity relationship.

10.1021/jm701301m
Published on Web 03/26/2008

each compound's output to that of known fluorophores. In addition to referencing the sample's fluorescence intensity to calibration fluorophore standards, we introduced an additional dimension to the study by profiling each compound at a series of concentrations, akin to the quantitative high-throughput screening (qHTS) approach.[26] We show that with this type of concentration−response-based profiling, one can derive brightness or potency measures of each compound with respect to known fluorophores in a manner where spurious light interferences (such as scatter and reflection by dust particles) are distinguished from sample fluorescence. The resulting detailed profile identified novel compounds with native fluorescence within each of the emission regions explored and provides detailed information on small-molecule scaffolds that may interfere with fluorescence-based assay results.

Experimental Section

Reagents. AlexaFluor 350, AlexaFluor 488, AlexaFluor 647 (all as carboxylic acids succinimidyl esters), and Texas Red were procured from Invitrogen (Carlsbad, CA). Fluorescein isothiocyanate, 4-methyl umbelliferone (4-MU), resorufin, and rhodamine were purchased from Sigma-Aldrich. Compound libraries and calibration fluorophores were dissolved in ACS grade DMSO (Fisher Scientific).

Compound Library. The 71 391-member library comprised two main subsets: 63 013 compounds from the NIH MLSMR (www.mli.nih.gov), prepared as 10 mM stock solutions in 384-well plates and delivered by Galapagos Biofocus DPI (South San Francisco, CA, http://mlsmr.glpg.com), and NCGC internal exploratory collection of 8378 compounds, which consisted of several commercially available libraries of known bioactives (1280 compounds from Sigma-Aldrich (LOPAC1280 library), 1120 compounds from Prestwick Chemical Inc. (Washington, DC), 280 purified natural products from TimTec (Newark, DE), and 1980 compounds from the National Cancer Institute (the NCI Diversity Set)), as well as collections from other commercial and academic collaborators (three 1000-member combinatorial libraries from Pharmacopeia (Cranbury, NJ) and 718 compounds from Boston University Center for Chemical Methodology and Library Development). The compound library (7 μL each in 1536-well Greiner polypropylene compound plate) was prepared as DMSO solutions at initial concentrations ranging between 2 and 10 mM. Plate-to-plate (vertical) dilutions and 384-to-1536 compressions were performed on Evolution P3 dispense system equipped with a 384-tip pipetting head and two RapidStak units (Perkin-Elmer, Wellesley, MA). Additional details on the preparation of the compound library are provided elsewhere.[26,27]

Fluorophore Standard Plate. The wells in columns 1−4 of a Kalypsys polypropylene 1536-well compound plate were populated with standard solutions of fluorophore corresponding to the spectral region of interest. For example, solutions of AlexaFluor 350 were dispensed in the following wells: I1, J1, 3 mM; I2, J2, 300 μM; I3, J3, 30 μM; I4, J4, zero (DMSO); K1, L1, 3 μM; K2, L2, 900 nM; K3, L3, 300 nM; and K4, L4, zero (DMSO) (Figure 1). Pin-transfer of approximately 23 nL of DMSO solution into the 6 μL of buffer solution resulted in final concentrations of the fluorophore standards as follows: 10 μM, 1 μM, 100 nM, 10 nM, 3 nM, 1 nM, and zero. The arrangement of the standards on the plate was done in a manner designed to maximize the distance between similar-color fluorophores, so that the optical crosstalk from high-intensity wells to the neighboring dark wells is minimized.

Automated qHTS Profiling Protocol. The assay protocol is described in Table 1. Briefly, all measurements were performed in 100 mM Tris buffer, pH 8.0. Aliquots of 6 μL of buffer were dispensed into 1536-well Greiner black plates via Kalypsys bottlevalve dispenser (Kalypsys, San Diego, CA). Compounds and fluorophore standards (23 nL) were transferred via Kalypsys pin tool equipped with 1536 slotted pins (V&P Scientific, San Diego, CA).[28] The plates were incubated for 15 min at room temperature and then read on a ViewLux high-throughput charge-coupled device (CCD) imager (Perkin-Elmer, Wellesley, MA) at a total of 15 excitation, emission, and exposure settings (Table 1, steps 5−12). Compound libraries were plated as seven-point titrations as previously described,[26,27] and during screening, each compound set was run from lower to higher concentration. All screening operations were performed under reduced lighting on a fully automated Kalypsys robotic system containing one RX-130 and two RX-90 anthropomorphic robotic arms.

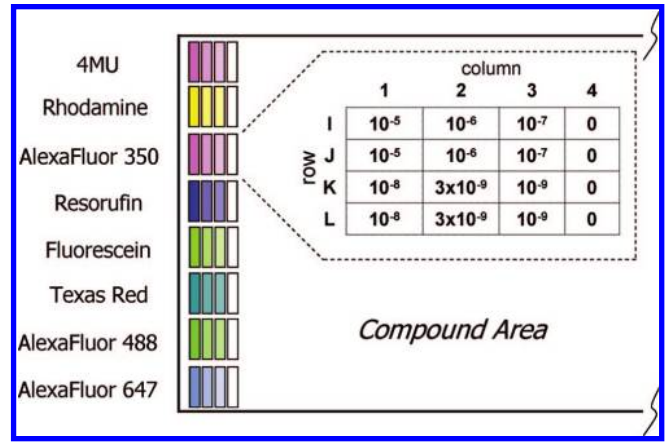

Figure 1. Plate map of fluorophore standards. Fluorescent standards (listed on the left) are transferred by pin tool from the 1536-well control plate to the 1536-well assay plate (32 rows (A−AF) by 48 columns). In the assay plate, the standards occupy columns 1−3, column 4 is DMSO/buffer only, and columns 5−48 contain library compounds. In the assay, each fluorophore standard is at a final concentration shown in the figure inset. 4-MU, 4-methyl umbelliferone.

Table 1. Spectroscopic Fluorescent Profiling qHTS Protocol

step	parameter	value	description
1[a]	reagent	6 μL	100 mM Tris buffer (pH 8.0)
2[b]	compound	23 nL	compound library (2.4 nM–38 μM)
3[c]	control	23 nL	control plate
4[d]	time	15 min	RT incubation
5−12[e]	detector	multiple	ViewLux fluorescence intensity reads

[a] Black solid plates, single-tip dispense. [b] Pin tool transfer of compounds to assay plate (columns 5−48). [c] Pin tool transfer of calibration solutions of fluorophores to columns 1−4 of all assay plates. [d] Room temperature incubation in auxiliary hotel. [e] Fluorophore, ViewLux Settings: excitation filter wavelength (bandwidth) in nm, emission filter wavelength (bandwidth) in nm, ViewLux excitation energy (unitless), CCD exposure time ((5) 4-MU, 340 (30), 450 (20), 8,000, 10 s; (6) AlexaFluor 350, 340 (30), 450 (20), 8,000, 10 s; (7) Fluorescein, 480 (20), 540 (25), 1,000, 1 s; (8) AlexaFluor 488, 480 (20), 540 (25), 1,000, 1 s; (9) Rhodamine, 525 (20), 598 (25), 800, 2 s; (10) Resorufin, 525 (20), 598 (25), 800, 2 s; (11) Texas Red, 547 (8), 618 (8), 10,000, 5 s; and (12) AlexaFluor 647, 570 (10), 671 (8), 12,000, 15 s).

Data Treatment. The standard curves of fluorophores, present on each plate as six-point concentration series, were used to compute normalized fluorescence responses, termed fluorophore-equivalent concentrations (FECs), for each compound at each concentration. For example, the fluorescence response of a compound at a certain concentration in the 4-MU spectral region measured (excitation 360 nm, emission 450 nm) was correlated to the 4-MU standard curve generated on the same microtiter plate by using the six concentrations of 4-MU delivered out of the control plate. As a result of such correlation, a 4-MU FEC was assigned to that compound at that particular concentration. The ViewLux settings for measuring AlexaFluor 647 could not be optimized to achieve high sensitivity for this fluorophore, primarily because of the lack of appropriate filter set (a 570 nm excitation filter was used, which is significantly removed from the 650 nm excitation peak of the standard) and the fact that CCD-based plate readers are generally less sensitive to fluorophores in the far-red end of the visible spectrum. The calibration curves for AlexaFluor 647 used only three points as

opposed to the other seven fluorophores, which were calibrated with all six concentration points in almost every plate instance.

Self-Organizing Maps. The screened compound collection was clustered for chemical similarity by using the self-organizing map (SOM)[29] package SOM Toolbox (Adaptive Informatics Research Centre, Helsinki, Finland) with Daylight 1024-bit structural fingerprints (Daylight Chemical Information Systems, Inc., Santa Fe, NM). SOMs are well studied and widely used in diverse fields[30] for the reduction and 2D visualization of high-dimensional data, especially chemical structure space.[31,32] The computed FECs were then used to color the SOM for each spectral region as follows. For each cluster, the fraction of fluorescent compounds (maximum FEC $> 10^{-7}$ M) was compared to the library average fraction of fluorescent compounds, and a statistical significance (p value by using Fisher's Exact test) was calculated. SOM cluster colors were scaled by the negative log of the p values, such that clusters significantly enriched with fluorescent molecules were colored dark red, clusters significantly deficient in fluorescent molecules were colored dark blue, and clusters with either no fluorescent compounds or the library average fraction of fluorescent compounds were colored green.

HPLC Analyses. To further quantify the degree of fluorescence of the library, over 50 compounds were purchased and reanalyzed for purity and fluorescence emission at selected wavelengths via high-performance liquid chromatography (HPLC). The purity analysis was made by using liquid chromatography−mass spectrometry analysis on a Waters ACQUITY reverse phase UPLC System and 1.7 M BEH column (2.1 × 50 mm) by using a linear gradient in 0.1% aqueous formic acid (5% ACN in water increasing to 95% over 3 min). Compound purity was measured on the basis of peak integration from both UV/vis absorbance and evaporative light scattering detection, and compound identity was determined on the basis of mass analysis. A secondary analysis was performed on an Agilent 1100 LC system equipped with diode-array absorbance and fluorescence detectors and an Eclipse XDB-C18 column (2.1 × 100 mm) by using a linear gradient of Tris buffered to pH 6.5 with TFA (10% ACN in water increasing to 80% over 12 min), and compound fluorescence was monitored by using excitations at 360 and 495 nm and emission outputs at 455 and 520 nm.

Spectrofluorometry. Experiments to record the excitation and emission spectra of select compounds, diluted to 5 μM in 100 mM Tris pH 8.0, were performed on a Fluoromax-4 (Horiba Jobin Yvon, Edison, NJ) spectrofluorometer equipped with a single-cuvette sample holder. Spectra were recorded at room temperature in semimicro Spectrosil Far UV quartz 5 mm path length cuvette (Starna Cells, Atascadero, CA). Typically, the monochromator wavelength steps were set at 1 nm, and the integration time was 0.1 s. The excitation and emission slit widths were 2 nm.

Results and Discussion

Overview. Here, we report the generation of a comprehensive and robust data set of the fluorescent properties of all samples in several large and widely used screening libraries. In order to facilitate the broad use of these data in the interpretation of HTS results, we report the fluorescence as fluorophore equivalents based on commonly used HTS fluorescent probes and spectral filter sets. The profiles were assembled through a series of measurements designed to capture the majority of the UV/vis spectrum and in particular those spectral wavelengths utilized in typical HTS assays.[1] On the basis of filter availability and frequency of fluorophores reported in screening assays, we selected eight fluorophores as standards and utilized the high-speed CCD-based ViewLux imager in conjunction with filter and camera settings to cover the following regions of the UV/vis spectrum: 4-MU and AlexaFluor 350 were used for the UV and low-wavelength visible region (excitation 340 nm, emission 450 nm), fluorescein and AlexaFluor 488 covered the green portion of the visible spectrum (excitation 480 nm, emission 540 nm), whereas rhodamine, resorufin, and Texas Red were positioned in the middle and the red regions of the visible spectrum (excitation 547 nm, emission 598 nm for rhodamine and resorufin and excitation 547 nm, emission 618 nm for Texas Red). Lastly, AlexaFluor 647 (excitation 570 nm, emission 671 nm) represented a fluorophore at the far-red end of the visible spectrum, where relatively few HTS assays are currently being measured. Thus, 4-MU and AlexaFluor 350 served as standards to judge the compounds' fluorescent behavior in widely used assay systems such as NADH and NADPH generation/consumption, coumarin-based profluorescent phosphatase and protease substrates, and β-lactamase cellular reporter assays utilizing CCF4 as substrate, the latter being a cephalosporin derivative that contains coumarin and fluorescein moieties bridged by a lactam ring.[13,14] Fluorescein and AlexaFluor 488 represented another frequently utilized portion of the spectrum, where a very large number of fluorescein-based or fluorescein-related fluorophores are being used to configure fluorescence polarization enzymatic and binding assays. Various BODIPY fluorophores, as well as rhodamine and Texas Red themselves, are represented by the three red standards, rhodamine, resorufin, and Texas Red.

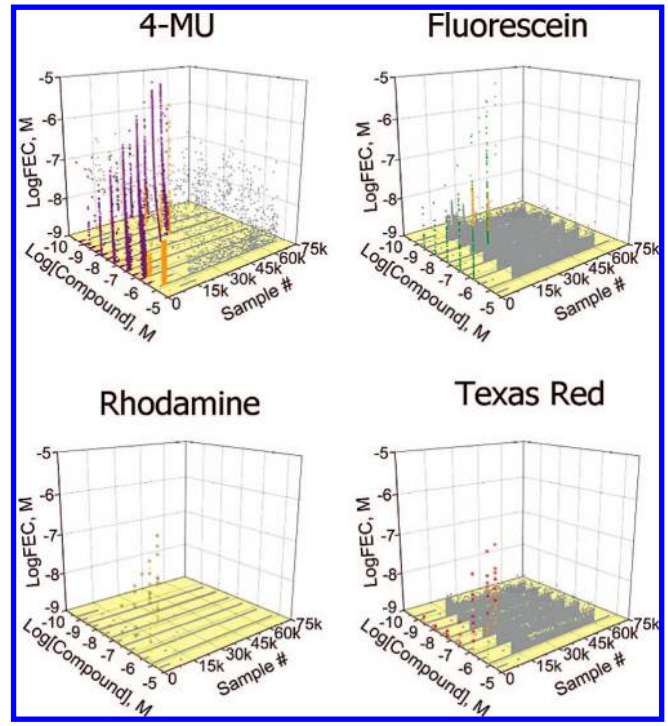

Figure 2. Cumulative spectroscopic profiling results for selected spectral regions. Data shown for the 4-MU, fluorescein, rhodamine, and Texas Red spectral regions. Shown are the FEC points for each compound at each concentration, the most fluorescent samples being presented first. Samples showing a strong concentration−response for the FEC values are colored in purple (4-MU), green (fluorescein), yellow open circles (rhodamine), or red (Texas Red). For each graph, inconclusive samples are shown in orange, and inactive samples, where no concentration−response was observed in the FEC, are shown in gray.

The qHTS spectroscopic profiling utilized a total of 476 1536-well assay plates, and fluorescent signals from the calibration wells remained stable throughput the screen (data not shown). In Figure 2, we present the entirety of concentration−response profiles collected across four wavelength regions. These plots also clearly illustrate the origin of potential false positives as spurious fluorescent wells from samples that do not show concentration-dependent response. Random contamination of either sample or assay wells with lint/dust particulates can often

Table 2. Number and Percentage of Compounds (out of 71 391 Tested) Displaying Fluorescence Equivalents Equal to or Exceeding 100 and 10 nM Standards

fluorophore standard	>10 nM	% of library	>100 nM	% of library
4-MU	3498	4.90	1306	1.83
AlexaFluor 350	3643	5.10	138	1.92
AlexaFluor 488	23	0.03	7	0.01
fluorescein	119	0.17	31	0.04
resorufin	7	0.01	3	0.004
rhodamine	7	0.01	3	0.004
Texas Red	8	0.01	1	0.001
AlexaFluor 647	0	0	0	0

lead to wells of high signal in fluorescent HTS assays;[1,13,14] however, such artifacts are rarely seen with red-shifted fluorophores. By isolating and counting the single-occurrence fluorescent wells (FEC > 10^{-8} M) within a compound concentration series, we were able to obtain an estimate of the particulate effect under these experimental conditions. Within the 4-MU and AlexaFluor 350 region, the effect was noted in approximately 400 samples, whereas within the fluorescein and AlexaFluor 488 window, spurious fluorescence affected approximately 20 samples, and no effect was observed in the red-shifted regions. Although the relative proportion of particulate-affected wells is expected to vary from facility to facility and indeed between experiments within the same laboratory, it is noteworthy that the fraction of affected samples in our experiment was relatively low (<0.1% of total compounds tested in the blue region). These data also illustrate the utility of the qHTS approach for such profiling studies; indeed, attempting to generate a fluorescent profile for blue-shifted fluorophores by using a single concentration would be misleading because of these sporadic interferences.

A determination of the number and percentages of small molecules that yield FECs exceeding either the 100 or 10 nM concentrations of 4-MU, AlexaFluor 350, fluorescein, Alexa Fluor 488, rhodamine, resorufin, Texas Red, or AlexaFluor 647 within the library of 71 391 compounds was made (Table 2). The total numbers reflect compounds which fluoresce at the highest concentration tested, with the trend supported by at least one adjacent lower-concentration point. In addition to the multipoint fluorescent actives reported in Table 2, we observed 2871 compounds in the blue and 221 compounds in the fluorescein regions for which only the maximum-concentration tested registered a signal above the 10^{-8} M FEC threshold, whereas the rest of the concentration−response was flat. We have elected to call these inconclusive actives because of the uncertainty associated with using only the maximum-concentration value. The majority of these inconclusive actives are likely compounds the fluorescence of which is weak and therefore only detectable at the highest concentration, whereas others may be spurious particulate-related interferences. Assuming accurate estimates of dust interference, we can state that out of the 2871 inconclusive actives, at least 2400 are not associated with particulate-based artifacts. However, the data do not allow us to discriminate dust versus top-concentration fluorescence assignments for individual concentration series.

Our data, freely accessible in PubChem under Assay IDs 587, 588, 590, 591, 592, 593, and 594, are in general agreement with the recent PubChem deposition of data on blue spectral fluorescence of MLSMR compounds at a single (10 μM) concentration. In that assay, performed at the Southern Research Molecular Libraries Screening Center (SRMLSC), a preread was collected at excitation and emission wavelengths of 339 and 460 nm, respectively, and each compound's fluorescence was

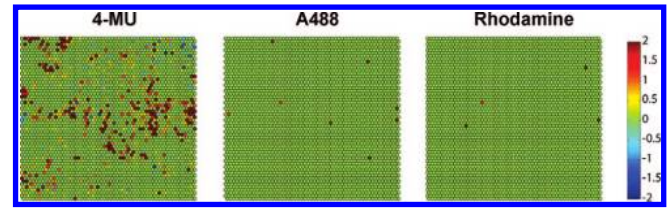

Figure 3. Compound library self-organizing map with fluorescent activity overlay. SOM of library profiled against 4-MU (left), Alexa Fluor 488 (middle), and rhodamine (right). The hexagons (clusters) in each SOM are colored by the enrichment level of fluorescent compounds in that cluster with respect to a fluorophore. The statistical significance of the enrichment is measured by the p value from a Fisher's exact test. The color is scaled by the negative log of the p values, such that a cluster with a dark red (blue) color is significantly enriched (deficient) in fluorescent compounds when compared to the library average, respectively, and a green cluster either has no fluorescent compounds or its fraction of fluorescent compounds is not different from the library average.

compared with that of the NADH cofactor present in the enzyme assay mixture. Out of 65 420 compounds tested, 3590 (5.5%) scored as fluorescent in the SRMLSC assay (comparable to the 4.9% (with 4-MU) and 5.1% (with AlexaFluor 350) that were observed in the profile described here). Approximately two-thirds of the SRMLSC actives were also identified in our profiling, and the overlap of inactives was approximately 95% (data not shown). The concurrence of these results, despite significant differences in experimental parameters (e.g., number of concentration points tested, fluorophore used as comparison, buffer conditions, plate reader type, and plate density), suggests that the profiling reported here will be generally useful when applied to screening results in other laboratories and under other conditions.

The high percentage of compounds that fluoresce within the shorter wavelengths associated with 4-MU and AlexaFluor 350 confirms the generally accepted notion that greater fluorescence interference is observed with blue-shifted probes and highlights the need for such profiling data as a component in the evaluation of screening data. The results are consistent with the fact that a small level of conjugation can confer fluorescent properties to small molecules with common substructures. Overall, longer conjugated paths and larger ring systems were observed as the spectral region shifted toward red (see examples in Supporting Information, Figure S1).

The compounds that represent the most fluorescent molecules within this and any collection at these wavelengths will certainly present a relevant concern for high-throughput screens where the reporter fluorophore is utilized at low levels, generally below 1 μM. On the opposite end of the spectrum, we found a very limited number of compounds fluorescent in the Texas Red region and none that could be considered fluorescent in the AlexaFluor 647 region. The lack of fluorescent compounds identified in the farthest-red end of the spectrum could be partially due to the limitations of the CCD-based imager and the filter set used to address this fluorophore, which resulted in a relatively poor limit of detection of slightly over 100 nM.

In order to probe the relationship between chemical structure and fluorescence, the compound collection used in this study was clustered by using a SOM algorithm based on similarity in their Daylight structural fingerprints for the three spectral regions shown in Figure 3. In this figure, each hexagon represents a cluster of structurally similar compounds. The color of each hexagon represents the enrichment level of fluorescent compounds for that cluster. The figure clearly shows that a wide variety of compounds in the collection are fluorescent in the

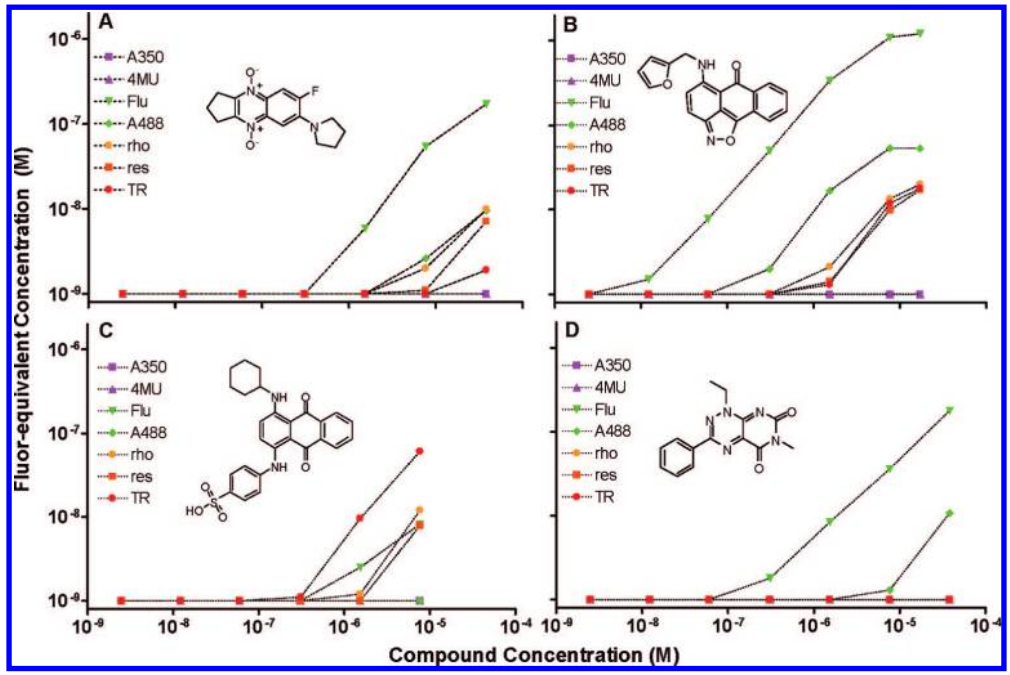

Figure 4. FEC-compound titration plot with examples. Clear SAR trends are observed of structures showing their fluorescence-equivalence with specific fluorophores and titration curves from primary screen. Shown are (A) a quinoxaline 4,9-dioxide, (B) an anthraisoxazol-6-one, which are both broadly fluorescent, (C) a dihydroanthracene-9,10-dione, which is primarily fluorescent in the red, and (D) a pyrimido triazine dione, which is strictly fluorescent in the fluorescein region.

4-MU spectral neighborhood, whereas relatively few structural clusters are fluorescent in the orange/red region (rhodamine). Clear SAR trends are observed for 4-MU fluorescent compounds because adjacent clusters (which are themselves structurally related) tend to group together to form contiguous regions of red-colored clusters in the SOM (Figure 3, left panel). The blue-colored clusters, significantly deficient in fluorescent compounds, are sparsely distributed and may indicate that the rare fluorescent compounds in these clusters are actually contaminated with a fluorescent impurity or a fluorescent R-group not associated with the cluster definition. Representative scaffolds and individual compounds were derived from the clusters for each spectral region (see Supporting Information, Figure S1). In general, longer conjugated frameworks and larger ring systems were enriched when going from blue to red spectral regions. However, it is beyond the scope of this study to define detailed structure−activity relationship trends that could be used to predict compound fluorescence based on structure, despite the fact that the SOMs clearly demonstrate that structurally related neighbors of fluorescent molecules also tend to be fluorescent. Therefore, despite the unprecedented size of this profiling data set, assignment of compound fluorescence must for now remain an empirical process.

At longer wavelengths (e.g., >550 nm), there is a precipitous drop in the number and percentage of compounds that natively fluoresce at a level that would confer relevance to most screening assays. These findings parallel the relative scarcity of red-shifted fluorophores and the wealth of choices in the blue/green region. Interestingly, among the small number of compounds fluorescent beyond the fluorescein region were several naturally fluorescent bioactives, such as daunomycin, topotecan, and riboflavin. The profiling revealed numerous core structures corresponding to known, fluorescent scaffolds; it also identified several fluorescent small molecules with structures not directly related to any well-characterized fluorophores yet containing a fittingly conjugated system as demonstrated by representative examples in Figure 4.

Novel Fluorophores. The present profile additionally allows evaluation of the library for novel fluorescent structures. Interestingly, several novel scaffolds were fluorescent in at least one spectral sector. Two of the most intriguing structures were 6-amino-2-ethyl-8-phenethyl-2,3,8,8a-tetrahydroisoquinoline-5,7,7(1*H*)-tricarbonitrile and (*Z*)-2-oxo-3-(1,3,3-trimethylindolin-2-ylidene)propyl-2-(5-phenyl-2*H*-tetrazol-2-yl) acetate, the excitation and emission spectra of which, derived from independently sourced samples, are shown in Figure 5. Neither structure contains the significant degree of conjugation that is typically associated with fluorescent compounds, nor is there direct overlap with any core moiety common to known fluorophores. Note, while the fluorescent signal found during LC analysis of these compounds was associated with the compound peak, we have not fully characterized the fluorescent nature of these compounds.

A consistent scaffold that had fluorescent properties was the 2-cyano-*N*-methyl-2-(3-(substituted-amino)quinoxalin-2-yl)-substituted-amide (Table 3). Several quinoxalin−imidazolium substructures have recently been reported to fluoresce as a result of a charge transfer process.[33] The core structure contains a strongly basic 2-substituted amine moiety and a relatively acidic proton (the 2-position of the 3-oxoalkylnitrile moiety), which engender the latter with the ability to exist as a zwitterionic form that can induce intermolecular stacking and excimer formation.

Impurities. Impurities can plague a screening collection despite the great efforts frequently undertaken to ensure their integrity. It was therefore no surprise that a percentage of the library samples analyzed here contained impurities that conferred a degree of fluorescent character that was not associated with the cognate library small molecule. Among 50 fluorescent compounds subjected to reanalysis, we observed fluorescent impurities in five samples. An example is shown in Figure 6, where the core structure of the 2-(([1,2,4]triazolo[4,3-a]pyridin-3-ylthio)methyl)-1-ethyl-1*H*-benzo[d]imidazole-5-carboxylic acid (peak with strong UV absorbance at approximately 6 min) was

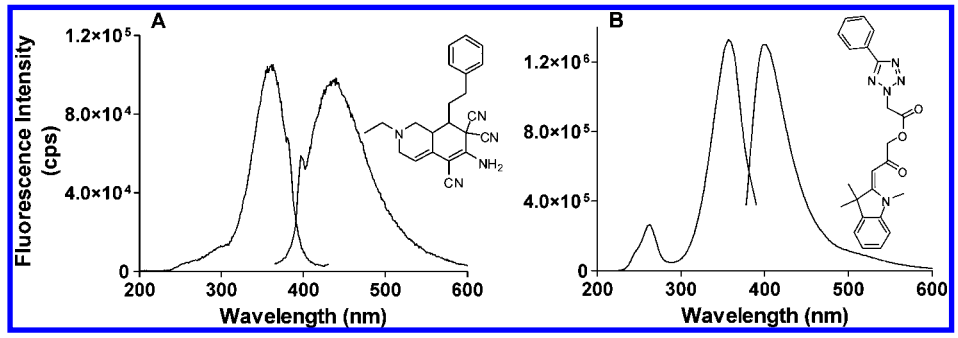

Figure 5. Excitation and emission spectra of novel fluorescent molecules.

Table 3. Structural Series and Fluorescent Equivalence of Novel Fluorophore with 2-Cyano-*N*-methyl- 2-(3-(substituted-amino)quinoxalin-2-yl)-substituted-amide Core

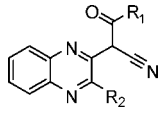

compound	R_1	R_2	fluorescein log(FEC)
1	benzyl amide	*N*-piperidine-3-carboxylic ethyl ester	−6.1
2	hexyl amide	pyrrolidin-1-yl	−6.1
3	pentyl amide	pyrrolidin-1-yl	−6.3
4	benzyl amide	pyrrolidin-1-yl	−6.4
5	pentyl amide	morpholin-1-yl	−6.3
6	cyclohexyl amide	*N*-piperidine-4-carboxylamide	−6.5
7	4-methoxybenzyl amide	pyrrolidin-1-yl	−6.5
8	cyclohexyl amide	*N*-piperidine-(4-(4-fluorophenyl))	−6.5
9	cyclopropyl amide	pyrrolidin-1-yl	−6.8
10	cyclopropyl amide	*N*-piperidine-(4-(4-styrylphenyl))	−6.9
11	phenethyl amide	piperidin-1-yl	−6.9
12	phenethyl amide	*N*,*N*-diethylamino	−6.9
13	benzo[*d*][1,3]dioxol-5-ylmethyl amide	2,6-dimethylmorpholin-1-yl	−7.0

not fluorescent at the excitation wavelengths of 360 and 495 nm and emission output at 455 and 520 nm (the blue and green regions where the original sample was fluorescently active). However, impurities that had minimal UV absorbance at 254 nm were noted to have a significant fluorescence emission (peaks at 9.3 and 14.3 min). Thus, less than 5% of the material in this sample appears to be the source of as much as 100% of the fluorescence. We note that relevant biochemical efficacy of a sample may be unrelated to the presence of a fluorescent impurity, and furthermore, impurities are likely to be inconsistently present. Thus, both enumeration and removal of fluorescent impurities from large collections will remain the focus of intense compound-management efforts.[34,35] We therefore advocate that profiles such as these be used to scrutinize, rather than necessarily eliminate, potential leads. Sample impurities may be temporally consistent when they originate from a certain synthetic route but may also be temporally variable by virtue of decomposition. Library members derived from final-stage coupling reactions with highly conjugated agents, such as HATU (2-(1*H*-7-azabenzotriazol-1-yl)-1,1,3,3-tetramethyl uronium hexafluorophosphate), are candidates for such effects if improperly purified. Furthermore, compound degradation via mechanisms producing higher levels of conjugation (such as Grob fragmentations) may result in fluorescent impurities derived directly from the library sample, and degradation products will undoubtedly increase in concentration over time. Again, these effects are singular, and generalizations are not employable, making profiles of individual compound libraries highly useful.

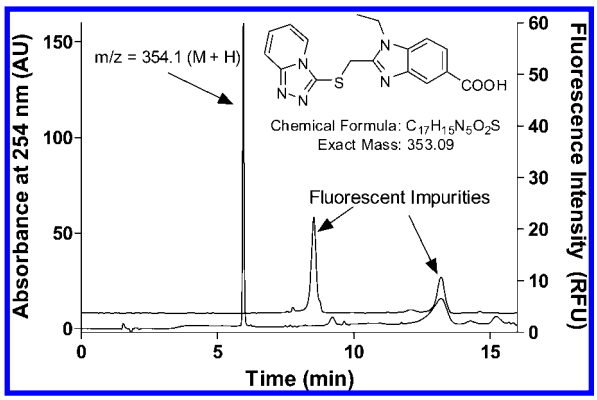

Figure 6. HPLC analysis of nonfluorescent compound containing a fluorescent impurity.

Utilization of Profiling Data. To be maximally useful, the database of spectroscopic properties reported here should allow the triaging of hits from HTS campaigns, especially when the use of a blue-shifted assay signal leads to the identification of an excessively large number of putative actives. To model this utility, we used the fluorescence profiles defined here to retrospectively evaluate the results of 39 NCGC screens comprising a broad range of in vitro and cell-based biology and detection platforms (fluorescence, absorbance, and luminescence). We asked the following question: are compounds identified by the profile as fluorescent within a certain spectral region going to be overrepresented among the actives in assays utilizing light detection relevant to that particular region? Figure 7 shows the fraction of compounds identified as active in each of the 39 assays which are also expected to have been fluorescent on the basis of the detection wavelength used, from UV/blue on the left of each panel to red-shifted toward the middle (assays 23 and 24) and wavelength-neutral assays on the right. Thus, in Figure 7A, we show the UV-fluorescent compounds identified as active in each of the 39 assays as a fraction of all actives within that same assay. Analogously, in Figure 7B, we present the fractions of all actives represented by green-fluorescent active compounds, and we do likewise for the rhodamine (Figure 7C) and Texas Red (Figure 7D) regions. Blue-fluorescent compounds comprise 5% of the library, but in assays utilizing or affected by blue light, they represent almost 50% of the identified actives, which is equivalent to nearly 10-fold enrichment (assays 1−3 in Figure 7A). However, in assays with detection outside the blue-end of the spectrum (assay 5 and beyond), their percent of the active compounds is close to their fraction of the total library. Similar enrichment is evident in

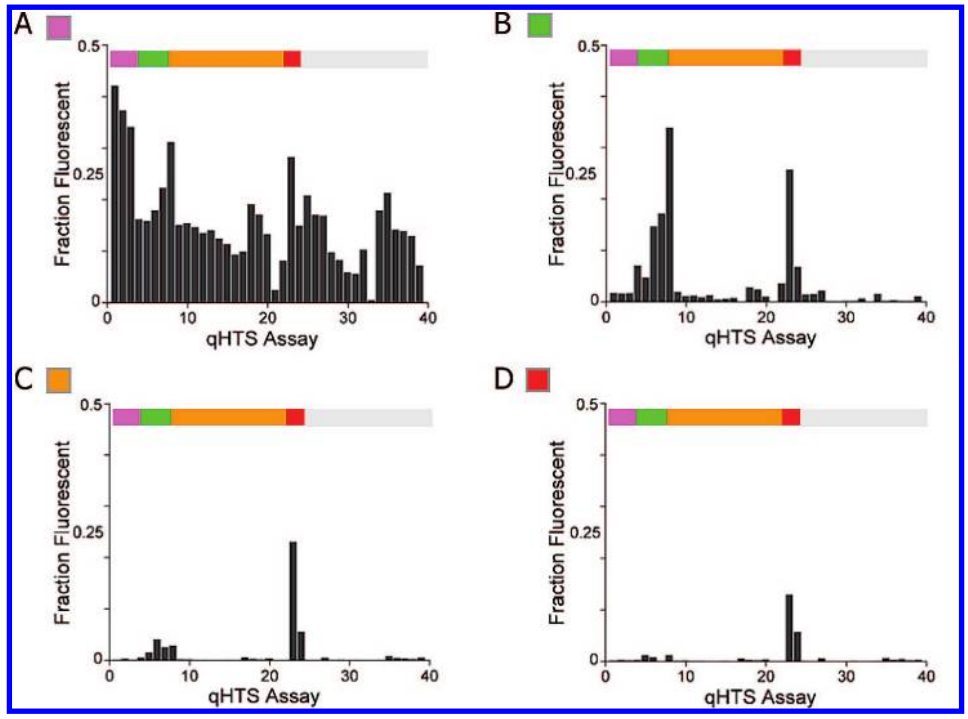

Figure 7. Enrichment of fluorescent compounds among the actives in wavelength-relevant regions. A fluorescence profile across 39 qHTS assays is shown, where the fraction of fluorescent compounds out of all actives identified in each screen is plotted for the library members fluorescent in 4-MU (A), fluorescein (B), rhodamine (C), and Texas Red (D) spectral regions. Assays are ordered by the spectral region being measured, ranging from blue (assay 1) to red (assay 24), and assays considered to be wavelength-neutral (assays 25−39, gray overhead bar).

the fluorescein region (Figure 7B), where green-fluorescent compounds represent a large fraction of the actives detected in the assays affected by green light (assays 6−10) but a minute fraction of the actives in other screens. Likewise, red-fluorescent compounds (Figure 7C and D) preferentially appear as hits in the two assays utilizing or affected by red light (assays 23 and 24). The assays represented by numbers 10−20 did utilize light in the 550 nm region but were significantly less affected by fluorescence interference because of a combination of high concentration of assay chromophore/fluorphore and the collection of time course data. It is therefore likely that for each assay, the proportion of active compounds that fluoresce at the assay readout wavelength and are above their prevalence in the overall library has no biological basis for activity. These results demonstrate how choice of assay readout can lead to an enrichment of molecules spectrally active in that region, and how the spectral profiles generated here can be used to identify them as suspect. Furthermore, the data presented here suggest that shifting the detection wavelength of HTS assay readout beyond 500 nm would be beneficial in reducing fluorescence-associated nonbiologically relevant positives.

These results suggest that the database of native compound fluorescence should be relevant to the evaluation of HTS results; therefore, we next tested this utility directly by using the profiling data to evaluate actives from two recent NCGC primary screens. The first, a qHTS for inhibitors of an oxidoreductase that utilized a fluorescent output based upon the conversion of the nonfluorescent NAD^+ cofactor to its UV-fluorescent reduced counterpart, NADH, revealed a series of substituted 2-imino-1*H*-dipyrido[1,2-a:2′,3′-d]pyrimidin-5(2*H*)-ones that exhibited a broad range of potencies. On the basis of their activity range and synthetic optimization potential, these compounds were considered leads of interest. However, because the assay output was based upon generation of blue-shifted fluorescence, we compared the oxidoreductase activity of these compounds with their 4-MU and Alexa 350 fluorescence profiling FECs. Among the 52 compounds that shared this core structure, 28 were scored as active in the oxidoreductase screen, and a considerable percentage (23 out of 28, or ∼82%) of these showed high fluorescent equivalence at both 4-MU and Alexa 350. Conversely, the 24 structural class members deemed inactive had far weaker fluorescent equivalence levels (Figure 8). On the basis of these data, follow-up studies were performed; they confirmed that the active compounds were indeed fluorescent false positives, and the structural series was abandoned.

The second primary-screen data set we analyzed by using the profiling data comprised putative activators of β-glucocerebrosidase identified in a pilot screen which utilized a 4-MU-containing profluorescent substrate. Four activators were identified in the screen and were analyzed with respect to their FEC in the screen-relevant 4-MU region (Figure 9); among these, only one compound (Figure 9, solid triangle) showed no FEC activity. The activity of these four compounds was then evaluated by HPLC analysis, by assaying for both the expected change in substrate−product ratio and the appearance of extra compound peaks suggestive of impurities.[36] The compound with no FEC (Figure 9, solid triangle) enhanced product formation and was devoid of extra peaks in the HPLC analysis, confirming this compound as an enzyme activator. Conversely, all three compounds with significant FECs failed to enhance product formation and/or contained highly fluorescent impurities; these were therefore categorized as nonbiological actives (i.e., reproducibly active in the assay but for reasons not associated with target-biology activity).

Thus, the results generated here are useful in both retrospective and prospective analyses of primary-screening data. However, it must be stressed that, in our view, these profiles should be used as means to scrutinize lead series rather than as an absolute filter of actives. Inherently fluorescent compounds have a long history of utility in biology and medicine,[37,38] and this assay interference property should not preclude their use; furthermore, subtle differences in assay conditions may affect

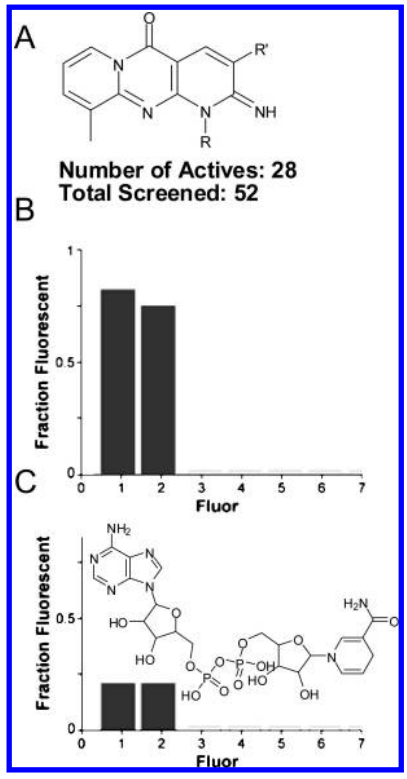

Figure 8. FEC−SAR-guided series triage. (A) Survey of substituted 2-imino-1*H*-dipyrido[1,2-a:2′,3′-d]pyrimidin-5(2*H*)-ones identified from an oxidoreductase screen by utilizing an NADH (structure shown in panel C) fluorescence measurement. (B) Over 80% of putative actives within the screen had high FEC relative to 4-MU (1) and AlexaFluor 350 (2) and showed low FEC in flourescein (3), A488 (4), rhodamine (5), resorfun (6), and Texas Red (7). (C) Approximately 20% of the inactives demonstrated low FEC relative to 4-MU and AlexaFluor 350.

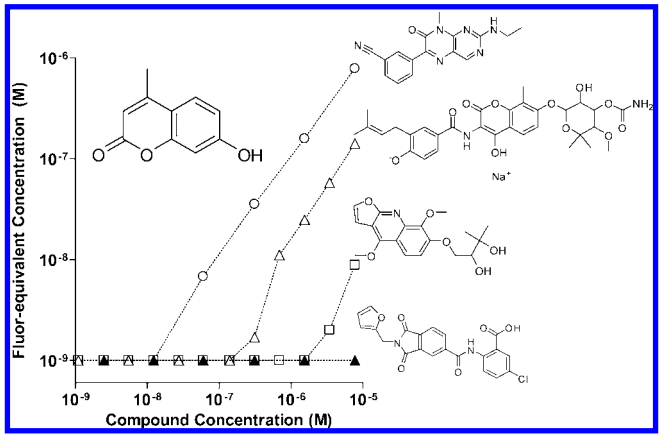

Figure 9. FEC−HPLC-guided sample triage. Spectroscopic fluorescent profiles of four putative glucocerebrosidase activators identified in a 4-MU-based (structure in upper left corner) fluorogenic assay. Only the compound with flat fluorescent response (solid triangle) was later confirmed as an activator via independent HPLC analysis.

compound fluorescence (such as the dramatic drop-off in fluorescein's fluorescence upon transition from pH > 7.0 to slightly acidic pH because of the protonation-induced change in π-conjugation).

Conclusions

The primary role of HTS is the discovery of small molecules that specifically modulate biological processes. Natively fluorescent compounds may masquerade as legitimate modulators of protein and cell functions and consequently lead to the futile pursuit of biologically inactive compounds in chemical genomics and drug-development campaigns. Thus, methods to efficiently eliminate these compounds from follow-up consideration are urgently needed. The profiles reported here identify a large number of small molecules with fluorescence properties that overlap with those of commonly used fluorophores. The prevalence of both sample-dependent and spurious (i.e., particulate-related) fluorescence is the greatest at blue-shifted wavelengths and decreases with increasing wavelengths; library compounds with spectra that overlap with those of fluorophores having bathochromic shifts beyond 550 nm are rare.

Our findings indicate that, whenever possible, HTS assays should utilize readouts with red-fluorescent signal outputs, because this will limit the prevalence of fluorescent interference. We note that even a relatively minor assay wavelength-shift from the UV (coumarin-type labels) to the fluorescein region (FITC and related labels) can carry a significant benefit in HTS settings because it will lead to a dramatic reduction in interference from both library members and dust/lint particulates. Unfortunately, because of both limited structure−fluorescence correlation and stochastic occurrence of fluorescent impurities in individual compound samples, it is currently not possible to reliably predict sample fluorescence. Profiling of an even larger number of diverse compounds, correlated with analytical data over the lifetime of an individual sample, may improve this predictability. Interestingly, fluorescence profiling of compound libraries can lead to the identification of novel fluorescent structures that might have potential as new fluorophores. Although identification of fluorescent compounds will remain an empirical task, the profiling reported in this study should enable accurate deprioritization of fluorescent samples identified in screens and allow researchers using these samples to focus quickly on bona fide actives.

The combination of concentration−response screening (qHTS) and multiwavelength spectral data acquisition has allowed us to generate what we believe is the most comprehensive fluorescence-profiling data set assembled to date. We have additionally profiled the NCGC chemical library for aggregation-based inhibition[9] and for inhibitors of luciferase.[10] Taken together, these profiles should provide a useful counterscreen database for the openly available bioactivity data deposited within PubChem, allowing facile evaluation of assay actives and minimizing costly and time-consuming follow-up efforts on irrelevant activity, thus increasing the efficiency of lead development.

Acknowledgment. This research was supported by the Molecular Libraries Initiative of the NIH Roadmap for Medical Research and the Intramural Research Program of the NHGRI, NIH. We thank S. Michael, A. Yasgar, and C. Klumpp for assistance with library preparation and automated screening.

Supporting Information Available: Representative scaffolds and individual compounds based on primary FEC data. This material is available free of charge via the Internet at http://pubs.acs.org.

References

(1) Inglese, J.; Johnson, R. L.; Simeonov, A.; Xia, M.; Zheng, W.; Austin, C. P.; Auld, D. S. High-throughput screening assays for the identification of chemical probes. *Nat. Chem. Biol.* **2007**, *3* (8), 466.
(2) Archer, J. R. History, evolution, and trends in compound management for high throughput screening. *Assay Drug Dev. Technol.* **2004**, *2* (6), 675–81.
(3) Walsh, D. P.; Chang, Y. T. Chemical genetics. *Chem. Rev.* **2006**, *106* (6), 2476–530.

(4) Lipinski, C. A.; Lonbardo, F.; Dominy, B. W.; Feeney, P. J. Experimental and computational approaches to estimate solubility and permeability in drug discovery and development settings. *Adv. Drug Delivery Rev.* **1997**, *23*, 3–25 .
(5) Proudfoot, J. R. Drugs, leads, and drug-likeness: An analysis of some recently launched drugs. *Bioorg. Med. Chem. Lett.* **2002**, *12* (12), 1647–50.
(6) Rishton, G. M. Nonleadlikeness and leadlikeness in biochemical screening. *Drug Discovery Today* **2003**, *8* (2), 86–96.
(7) Roche, O.; Schneider, P.; Zuegge, J.; Guba, W.; Kansy, M.; Alanine, A.; Bleicher, K.; Danel, F.; Gutknecht, E. M.; Rogers-Evans, M.; Neidhart, W.; Stalder, H.; Dillon, M.; Sjogren, E.; Fotouhi, N.; Gillespie, P.; Goodnow, R.; Harris, W.; Jones, P.; Taniguchi, M.; Tsujii, S.; von der Saal, W.; Zimmermann, G.; Schneider, G. Development of a virtual screening method for identification of frequent hitters in compound libraries. *J. Med. Chem.* **2002**, *45* (1), 137–42.
(8) Crisman, T. J.; Parker, C. N.; Jenkins, J. L.; Scheiber, J.; Thoma, M.; Kang, Z. B.; Kim, R.; Bender, A.; Nettles, J. H.; Davies, J. W.; Glick, M. Understanding false positives in reporter gene assays: In silico chemogenomics approaches to prioritize cell-based HTS data. *J. Chem. Inf. Model* **2007**, *47* (4), 1319–27.
(9) Feng, B. Y.; Simeonov, A.; Jadhav, A.; Babaoglu, K.; Inglese, J.; Shoichet, B. K.; Austin, C. P. A high-throughput screen for aggregation-based inhibition in a large compound library. *J. Med. Chem.* **2007**, *50* (10), 2385–90.
(10) Auld, D. S.; Johnson, R. L.; Southall, N.; Jadhav, A.; Simeonov, A.; Austin, C. A.; Inglese, J. Characterization of a large chemical library for luciferase activity. *J. Med. Chem. 51*, 2372–2386.
(11) Beasley, J. R.; Dunn, D. A.; Walker, T. L.; Parlato, S. M.; Lehrach, J. M.; Auld, D. S. Evaluation of compound interference in immobilized metal ion affinity-based fluorescence polarization detection with a four million member compound collection. *Assay Drug Dev. Technol.* **2003**, *1* (3), 455–9.
(12) Turconi, S.; Shea, K.; Ashman, S.; Fantom, K.; Earnshaw, D. L.; Bingham, R. P.; Haupts, U. M.; Brown, M. J.; Pope, A. J. Real experiences of uHTS: A prototypic 1536-well fluorescence anisotropy-based uHTS screen and application of well-level quality control procedures. *J. Biomol. Screening* **2001**, *6* (5), 275–90.
(13) Kunapuli, P.; Ransom, R.; Murphy, K. L.; Pettibone, D.; Kerby, J.; Grimwood, S.; Zuck, P.; Hodder, P.; Lacson, R.; Hoffman, I.; Inglese, J.; Strulovici, B. Development of an intact cell reporter gene beta-lactamase assay for G protein-coupled receptors for high-throughput screening. *Anal. Biochem.* **2003**, *314* (1), 16–29.
(14) Oosterom, J.; van Doornmalen, E. J.; Lobregt, S.; Blomenrohr, M.; Zaman, G. J. High-throughput screening using beta-lactamase reporter-gene technology for identification of low-molecular-weight antagonists of the human gonadotropin releasing hormone receptor. *Assay Drug Dev.Technol.* **2005**, *3* (2), 143–54.
(15) Hodder, P.; Cassaday, J.; Peltier, R.; Berry, K.; Inglese, J.; Feuston, B.; Culberson, C.; Bleicher, L.; Cosford, N. D.; Bayly, C.; Suto, C.; Varney, M.; Strulovici, B. Identification of metabotropic glutamate receptor antagonists using an automated high-throughput screening system. *Anal. Biochem.* **2003**, *313* (2), 246–54.
(16) Grant, S. K.; Sklar, J. G.; Cummings, R. T. Development of novel assays for proteolytic enzymes using rhodamine-based fluorogenic substrates. *J Biomol. Screening* **2002**, *7* (6), 531–40.
(17) Feliciano, J.; Liu, Y.; Daunert, S. Novel reporter gene in a fluorescent-based whole cell sensing system. *Biotechnol. Bioeng.* **2006**, *93* (5), 989–97.
(18) George, J.; Teear, M. L.; Norey, C. G.; Burns, D. D. Evaluation of an imaging platform during the development of a FRET protease assay. *J. Biomol. Screening* **2003**, *8* (1), 72–80.
(19) Turek-Etienne, T. C.; Small, E. C.; Soh, S. C.; Xin, T. A.; Gaitonde, P. V.; Barrabee, E. B.; Hart, R. F.; Bryant, R. W. Evaluation of fluorescent compound interference in 4 fluorescence polarization assays: 2 kinases, 1 protease, and 1 phosphatase. *J. Biomol. Screening* **2003**, *8* (2), 176–184.
(20) Huss, K. L.; Blonigen, P. E.; Campbell, R. M. Development of a transcreenerTM kinase assay for protein kinase A and demonstration of concordance of data with a filter-binding assay format. *J. Biomol. Screening* **2007**, *12*, 578–584.
(21) Silverman, L.; Campbell, R.; Broach, J. R. New assay technologies for high-throughput screening. *Cur. Opin. Chem. Biol.* **1998**, *2* (3), 397–403.
(22) Valeur, B. *Molecular Fluorescence*, 3rd ed.; Wiley-VCH: Weinheim, 2006.
(23) Albani, J. R. *Structure and Dynamics of Macromolecules: Absorption and Fluorescence Studies*; Elsevier: Amsterdam, 2004.
(24) Lakowicz, J. R. *Principles of Fluorescence Spectroscopy*; Springer: Berlin, 2006.
(25) Haugland, R. P. *The Handbook — A Guide to Fluorescent Probes and Labeling Technologies*, 10th ed.; Molecular Probes, Inc.: Eugene, OR, 2006.
(26) Inglese, J.; Auld, D. S.; Jadhav, A.; Johnson, R. L.; Simeonov, A.; Yasgar, A.; Zheng, W.; Austin, C. P. Quantitative high-throughput screening: A titration-based approach that efficiently identifies biological activities in large chemical libraries. *Proc. Natl. Acad. Sci. U.S.A.* **2006**, *103* (31), 11473–8.
(27) Yasgar, A.; Shinn, P.; Jadhav, A.; Auld, D. S.; Michael, S.; Zheng, W.; Austin, C. P.; Inglese, J.; Simeonov, A. Compound management for quantitative high-throughput screening. *J. Assoc. Lab. Automation* **2008**, *13* (2), 79–89.
(28) Cleveland, P. H.; Koutz, P. J. Nanoliter dispensing for uHTS using pin tools. *Assay Drug Dev. Technol.* **2005**, *3* (2), 213–25.
(29) Kohonen, T. The self-organizing map. *Neurocomputing* **1998**, *21* (1–3), 1–6.
(30) Rabow, A. A.; Shoemaker, R. H.; Sausville, E. A.; Covell, D. G. Mining the National Cancer Institute's tumor-screening database: Identification of compounds with similar cellular activities. *J. Med. Chem.* **2002**, *45* (4), 818–40.
(31) Kaski, S.; Kangas, J.; Kohonen, T. *Neural Comp. Serv.* **1997**, *1*, 102–350.
(32) Zupan, J.; Gasteiger, J. *Neural Networks in Chemistry and Drug Design*, 2nd ed.; Wiley: Weinheim, 1999.
(33) Singh, N. J.; Jun, E. J.; Chellappan, K.; Thangadurai, D.; Chandran, R. P.; Hwang, I. C.; Yoon, J.; Kim, K. S. Quinoxaline-imidazolium receptors for unique sensing of pyrophosphate and acetate by charge transfer. *Org. Lett.* **2007**, *9* (3), 485–8.
(34) Shah, N.; Gao, M.; Tsutsui, K.; Lu, A.; Davis, J.; Scheuerman, R.; Fitch, W. L.; Wilgus, R. L. A novel approach to high-throughput quality control of parallel synthesis libraries. *J. Comb. Chem.* **2000**, *2* (5), 453–60.
(35) Popa-Burke, I. G.; Issakova, O.; Arroway, J. D.; Bernasconi, P.; Chen, M.; Coudurier, L.; Galasinski, S.; Jadhav, A. P.; Janzen, W. P.; Lagasca, D.; Liu, D.; Lewis, R. S.; Mohney, R. P.; Sepetov, N.; Sparkman, D. A.; Hodge, C. N. Streamlined system for purifying and quantifying a diverse library of compounds and the effect of compound concentration measurements on the accurate interpretation of biological assay results. *Anal. Chem.* **2004**, *76* (24), 7278–87.
(36) Simeonov, A.; Yasgar, A.; Klumpp, C.; Zheng, W.; Shafqat, N.; Oppermann, U.; Austin, C.; Inglese, J. Evaluation of micro-parallel liquid chromatography (μPLC) as a method for HTS-coupled actives verification. *Assay Drug Dev. Technol.* **2007**, *5* (6), 815–824.
(37) Chan, K. P.; Chu, K. O.; Lai, W. W.; Choy, K. W.; Wang, C. C.; Lam, D. S.; Pang, C. P. Determination of ofloxacin and moxifloxacin and their penetration in human aqueous and vitreous humor by using high-performance liquid chromatography fluorescence detection. *Anal. Biochem.* **2006**, *353* (1), 30–6.
(38) Perez-Ruiz, T.; Martinez-Lozano, C.; Sanz, A.; Bravo, E. Simultaneous determination of doxorubicin, daunorubicin, and idarubicin by capillary electrophoresis with laser-induced fluorescence detection. *Electrophoresis* **2001**, *22* (1), 134–8.

JM701301M